ELSEVIER

Journal of Computational and Applied Mathematics 119 (2000) 185–207

JOURNAL OF COMPUTATIONAL AND APPLIED MATHEMATICS

Filter bank algorithms for piecewise linear prewavelets on arbitrary triangulations

Michael S. Floater*, Ewald G. Quak, Martin Reimers

SINTEF Applied Mathematics, Post Box 124, Blindern, 0314 Oslo, Norway

Received 9 March 1999

Dedicated to Prof. Larry L. Schumaker on the occasion of his 60th birthday

Abstract

This paper studies algorithms for decomposition, reconstruction, and approximation based on piecewise linear prewavelets on bounded triangulations of arbitrary topology. Our key mathematical result is showing that the Schur complement of the associated two scale matrix is symmetric, positive definite, and well conditioned. Numerical examples suggest that thresholding based on prewavelets yields a smaller approximation error than when based on the simple 'Faber' decomposition scheme. © 2000 Elsevier Science B.V. All rights reserved.

Keywords: Wavelet spaces; Prewavelets; Piecewise linear splines; Triangulations; Local support; Filter bank algorithms; Thresholding

1. Introduction

Given a nested sequence of finite-dimensional linear spaces

$$S^0 \subset S^1 \subset S^2 \subset \cdots \tag{1.1}$$

and an associated sequence of complement spaces W^j, one obtains a decomposition

$$S^j = S^{j-1} \oplus W^{j-1} = S^0 \oplus W^0 \oplus \cdots \oplus W^{j-1}. \tag{1.2}$$

This simple framework is an example of *multiresolution* which is a basic idea underlying several numerical methods for PDEs such as multilevel finite element approximation [11] as well as wavelet techniques for signal and image processing [13].

* Corresponding author.

E-mail addresses: michael.floater@math.sintef.no (M.S. Floater), ewald.quak@math.sintef.no (E.G. Quak), martin.reimers@math.sintef.no (M. Reimers).

PII: S0377-0427(00)00378-2

Our specific interest is in decomposing the kind of data typical in scattered data approximation, terrain modelling, and geometric modelling. This was the motivation in [4–6] for choosing the S^j to be spaces of piecewise linear functions over a successively and uniformly refined triangulation. The spaces W^j were taken to be the *orthogonal* complements with respect to a suitable weighted L_2 inner product and a theory was developed for certain stable bases of the W^j of prewavelets with small support.

This paper concerns the practical aspects of using these prewavelets for decomposition, reconstruction, and approximation via thresholding. The main issue is *decomposition* which at each level j reduces to solving a linear system, whose matrix is the so-called *two-scale matrix* which has block form

$$\begin{pmatrix} I & Q_1^j \\ P_2^j & Q_2^j \end{pmatrix}. \tag{1.3}$$

Our main result is to show that the Schur complement matrix

$$\tilde{Q}_2^j := Q_2^j - P_2^j Q_1^j \tag{1.4}$$

is symmetric, positive definite and well conditioned. In fact its condition number is bounded independently of the level j, making it well suited to the conjugate gradient method.

In Section 2 we describe a general framework for decomposition and reconstruction with general bases. We subsequently focus in Section 3 on properties induced by choosing the nodal basis for the nested spaces S^j. In Section 4 we describe the prewavelet basis of W^j of [4] as well as discussing the alternative Faber basis. Section 5 is devoted to an analysis of the Schur complement matrix in (1.4).

We conclude the paper in Section 6 with numerical examples of decomposition, reconstruction, and thresholding both when applying our prewavelet basis and when using the Faber scheme. Our numerical results on thresholding show that the approximation error with respect to a fixed compression rate is generally smaller for prewavelets than for the Faber scheme.

2. Nested spaces over triangulations

In this section we describe a general framework for decomposition and reconstruction of piecewise linear functions over triangulations.

Let $[X]$ denote the convex hull of a subset X of $\mathbb{R}^2$. We will refer to the convex hull of three non-collinear points in $\mathbb{R}^2$ as a *triangle*. Let $\mathscr{T} = \{T_1, \ldots, T_M\}$ be a set of triangles and let $\Omega = \bigcup_{i=1}^M T_i$ be their union. We call $\mathscr{T}$ a `triangulation` if

(i) $T_i \cap T_j$ is either empty, a common vertex or a common edge, $i \neq j$,
(ii) the number of boundary edges incident on a boundary vertex is two,
(iii) Ω is simply connected.

By a *boundary vertex* or *boundary edge* of T we mean a triangle vertex or triangle edge contained in the boundary of Ω. All other vertices and edges are *interior vertices* and *interior edges*.

Given a triangulation $\mathscr{T}^0$ we next wish to consider its uniform refinement $\mathscr{T}^1$. By uniform refinement we mean that we divide each triangle in $\mathscr{T}^0$ into four congruent subtriangles and the set of all such subtriangles forms a triangulation $\mathscr{T}^1$; see Fig. 8 for an example. Similarly, we can refine

$\mathscr{T}^1$ to form $\mathscr{T}^2$, and so on. We let V^j be the set of vertices in $\mathscr{T}^j$, $j=0,1,2,\ldots$, and E^j the set of edges. Thus the V^j are nested,

$$V^0 \subset V^1 \subset V^2 \subset \cdots$$

and for $j \geqslant 1$, we regard the vertices in V^{j-1} as *coarse* vertices of V^j and those in $V_*^j := V^j \setminus V^{j-1}$ as *fine* vertices.

Next, let Ω be the union of triangles in $\mathscr{T}^0$ and let S^j be the linear space of all continuous functions over Ω which are linear over each triangle in $\mathscr{T}^j$. The space S^j is often referred to as $\mathscr{S}_1^0(\mathscr{T}^j)$ in the spline literature; for an overview of the theory of splines on triangulations see [10]. The spaces S^j are nested as in (1.1) and the dimension of S^j is $|V^j|$. The dimension of any complement space W^{j-1} in the sense of (1.2) is

$$\dim W^{j-1} = |V^j| - |V^{j-1}| = |V_*^j| = |E^{j-1}|.$$

By endowing the spaces in (1.2) with bases, decomposition and reconstruction can be viewed as changes of basis which can be described in terms of matrix equations.

Suppose that $\{\phi_v^j\}_{v\in V^j}$ is a basis for S^j, for $j=0,1,2,\ldots$ and $\{\psi_u^j\}_{u\in V_*^{j+1}}$ a basis for W^j. By choosing some (arbitrary) ordering of the vertices in V^j and V_*^{j+1}, we can regard these bases as row vectors

$$\Phi^j = (\phi_v^j)_{v\in V^j} \quad \text{and} \quad \Psi^j = (\psi_u^j)_{u\in V_*^{j+1}},$$

of size $|V^j|$ and $|V_*^{j+1}|$, respectively. Then any elements

$$f^j = \sum_{v\in V^j} f_v^j \phi_v^j \quad \text{and} \quad g^j = \sum_{u\in V_*^{j+1}} g_u^j \psi_u^j$$

in S^j and W^j, respectively can be written as

$$f^j = \Phi^j \boldsymbol{f}^j \quad \text{and} \quad g^j = \Psi^j \boldsymbol{g}^j, \tag{2.1}$$

where $\boldsymbol{f}^j$ is the column vector $(f_v^j)_{v\in V^j}$ of size $|V^j|$ and $\boldsymbol{g}^j$ the column vector $(g_u^j)_{u\in V_*^{j+1}}$ of size $|V_*^{j+1}|$ and the ordering of the elements in both vectors is the same as in Φ^j and Ψ^j.

Since S^{j-1} and W^{j-1} are subspaces of S^j, there exist two unique matrices

$$P^j = (p_{wv})_{w\in V^j, v\in V^{j-1}} \quad \text{and} \quad Q^j = (q_{wu})_{w\in V^j, u\in V_*^j} \tag{2.2}$$

of dimensions $|V^j| \times |V^{j-1}|$ and $|V^j| \times |V_*^j|$, respectively, such that

$$\Phi^{j-1} = \Phi^j P^j \quad \text{and} \quad \Psi^{j-1} = \Phi^j Q^j. \tag{2.3}$$

Suppose next that $f^j \in S^j$. Eq. (1.2) implies that there exist unique $f^{j-1} \in S^{j-1}$ and $g^{j-1} \in W^{j-1}$ such that

$$f^j = f^{j-1} + g^{j-1}. \tag{2.4}$$

Conversely, the sum of any two functions $f^{j-1} \in S^{j-1}$, and $g^{j-1} \in W^{j-1}$ is a function f^j in S^j. Substituting (2.1) into (2.4) yields a corresponding equation in the coefficient and basis vectors,

$$\Phi^j \boldsymbol{f}^j = \Phi^{j-1} \boldsymbol{f}^{j-1} + \Psi^{j-1} \boldsymbol{g}^{j-1}$$

and if we then substitute in (2.3) and use the fact that Φ^j is a basis for S^j we find

$$(P^j \; Q^j) \begin{pmatrix} \boldsymbol{f}^{j-1} \\ \boldsymbol{g}^{j-1} \end{pmatrix} = \boldsymbol{f}^j, \tag{2.5}$$

where the square *two scale matrix* $(P^j\ Q^j)$ is non-singular, of size $|V^j|$. Eq. (2.5) has two uses. It can be used for *decomposition*, i.e. for computing the coefficient vectors $\boldsymbol{f}^{j-1}$ and $\boldsymbol{g}^{j-1}$ from a given coefficient vector $\boldsymbol{f}^j$ and conversely, for *reconstruction*, or *composition*, i.e. for computing $\boldsymbol{f}^j$ from $\boldsymbol{f}^{j-1}$ and $\boldsymbol{g}^{j-1}$.

Applying decomposition or reconstruction successively for all levels $j=1,2,\ldots,m$, for some $m\geqslant 1$, leads to so-called *filter bank algorithms*. Filter bank algorithms calculate the coefficient vector of f^m from the coefficient vectors of f^0 and $g^0,\ldots,g^{m-1}$ in the equation

$$f^m = f^0 + g^0 + g^1 + \cdots + g^{m-1} \tag{2.6}$$

or the converse.

Algorithm A1. Decomposition.

Input: $m \in \mathbb{N}$ highest level,
$\boldsymbol{f}^m = (f^m_v)_{v\in V^m}$ coefficient vector of a given function $f^m \in S^m$.
(i) For each level $j = m, m-1,\ldots,1$, solve the linear system (2.5) for $\boldsymbol{f}^{j-1}$ and $\boldsymbol{g}^{j-1}$
Output: $\boldsymbol{g}^j$ $(j=0,1,\ldots,m-1)$ coefficient vectors of $g^0,\ldots,g^{m-1}$ in (2.6),
$\boldsymbol{f}^0$ coefficient vector of f^0 in (2.6).

Algorithm A2. Reconstruction.

Input: $m \in \mathbb{N}$ highest level
$\boldsymbol{g}^j$ $(j=0,1,\ldots,m-1)$ coefficient vectors of given functions $g^j \in W^j$,
$\boldsymbol{f}^0$ coefficients of a given function $f^0 \in S^0$.
(i) For each level $j=1,2,\ldots,m$, compute $\boldsymbol{f}^j$ from the matrix multiplications

$$\boldsymbol{f}^j = P^j\boldsymbol{f}^{j-1} + Q^j\boldsymbol{g}^{j-1}.$$

Output: $\boldsymbol{f}^m$ coefficient vector of f^m in (2.6).

A typical application of filter bank algorithms is data compression using thresholding (see [13]), numerical examples of which will be presented in Section 6. Here, a given function $f^m \in S^m$ is first decomposed into its components according to (2.6) by using Algorithm A1 and then the components $g^j \in W^j$ are replaced by functions $\hat{g}^j \in W^j$ by modifying their coefficients according to a particular strategy. We will base our examples on the so-called *hard thresholding*, which means that for some threshold $\varepsilon > 0$ (independent of j), we set, for $u \in V^{j+1}_*$,

$$\hat{g}^j_u = \begin{cases} g^j_u & \text{if } |g^j_u| \geqslant \varepsilon, \\ 0 & \text{otherwise.} \end{cases}$$

The ratio of the number of subsequent non-zero coefficients to the total number,

$$\sum_{j=0}^{m-1} |\{u \in V^{j+1}_* \colon \hat{g}^j_u \neq 0\}| \Big/ \sum_{j=0}^{m-1} |V^{j+1}_*|,$$

will be referred to as the *compression rate*.

Reconstruction by applying Algorithm A2 to the modified functions $\hat{g}^j$ then yields an approximant $\hat{f}^m \in S^m$ to the original function f^m given as

$$\hat{f}^m = f^0 + \hat{g}^0 + \hat{g}^1 + \cdots + \hat{g}^{m-1}.$$

The resulting approximation error is therefore

$$e^m = f^m - \hat{f}^m = \sum_{j=0}^{m-1} (g^j - \hat{g}^j). \tag{2.7}$$

3. The nodal basis

So far we have described algorithms for decomposition and reconstruction with respect to the spaces S^j and W^j without choosing specific bases Φ^j and Ψ^j. It is usually desirable in multiresolution to work with bases of functions with small support. Indeed such functions lead to *sparse* matrices P^j and Q^j in (2.3) which clearly makes both algorithms A1 and A2 more efficient. Thus, a natural choice of basis Φ^j for S^j is the *nodal basis*. This will be our approach in the remainder of the paper and we set $\phi_v^j(w) = \delta_{vw}$ for $w \in V^j$, so that $\operatorname{supp}(\phi_v^j) = M_v^j$, where

$$M_v^j = \bigcup_{v \in T \in \mathcal{T}^j} T.$$

The nodal basis has several consequences on the nature of the filter bank algorithms and the matrices involved, and it is appropriate to explore these consequences next, before later choosing specific complement spaces W^j and associated bases Ψ^j in Section 4.

First of all, the nodal basis is unique in having the fundamental property that

$$f = \sum_{v \in V^j} f(v)\phi_v^j, \quad \text{for all } f \in S^j. \tag{3.1}$$

This immediately gives us the *refinement equation* for the nodal basis

$$\phi_v^{j-1} = \sum_{w \in V^j} \phi_v^{j-1}(w)\phi_w^j = \phi_v^j + \frac{1}{2} \sum_{w \in V_v^j} \phi_w^j, \quad v \in V^{j-1}, \tag{3.2}$$

where V_v^j denotes the set of neighbours in V^j of a vertex v in V^j, and similarly,

$$\psi_u^{j-1} = \sum_{w \in V^j} \psi_u^{j-1}(w)\phi_w^j, \quad u \in V_*^j.$$

Thus the elements of both the matrices P^j and Q^j in (2.2) are merely evaluations of the bases Φ^j and Ψ^j respectively and we have

$$p_{wv} = \phi_v^{j-1}(w) = \left\{ \begin{array}{ll} 1 & \text{if } w = v, \\ \frac{1}{2} & \text{if } w \in V_v^j, \\ 0 & \text{otherwise} \end{array} \right\} \quad \text{and} \quad q_{wu} = \psi_u^{j-1}(w).$$

The structure of P^j in this case suggests that solving the linear system (2.5) can be reduced to solving a smaller linear system and making a back substitution. We first write the column vector $\boldsymbol{f}^j$

as

$$\boldsymbol{f}^j = \begin{pmatrix} \boldsymbol{f}_1^j \\ \boldsymbol{f}_2^j \end{pmatrix},$$

whose components are the column vectors $\boldsymbol{f}_1^j = (f_v^j)_{v\in V^{j-1}}$ and $\boldsymbol{f}_2^j = (f_u^j)_{u\in V_*^j}$ (with the same ordering as in Φ^j and Ψ^j, respectively). Then Eq. (2.5) can be expressed in the block form

$$\begin{pmatrix} I & Q_1^j \\ P_2^j & Q_2^j \end{pmatrix} \begin{pmatrix} \boldsymbol{f}^{j-1} \\ \boldsymbol{g}^{j-1} \end{pmatrix} = \begin{pmatrix} \boldsymbol{f}_1^j \\ \boldsymbol{f}_2^j \end{pmatrix}, \tag{3.3}$$

where the matrix P_2^j has elements

$$p_{wv} = \begin{cases} \frac{1}{2} & \text{if } w \in V_v^j, \\ 0 & \text{otherwise,} \end{cases} \tag{3.4}$$

for $w \in V_*^j$ and $v \in V^{j-1}$. Multiplying both the sides of Eq. (3.3) by the matrix

$$\begin{pmatrix} I & 0 \\ -P_2^j & I \end{pmatrix} \tag{3.5}$$

yields

$$\begin{pmatrix} I & Q_1^j \\ 0 & \tilde{Q}_2^j \end{pmatrix} \begin{pmatrix} \boldsymbol{f}^{j-1} \\ \boldsymbol{g}^{j-1} \end{pmatrix} = \begin{pmatrix} \boldsymbol{f}_1^j \\ \boldsymbol{f}_2^j - P_2^j \boldsymbol{f}_1^j \end{pmatrix}, \tag{3.6}$$

where $\tilde{Q}_2^j$ is the square matrix of dimension $|V_*^j|$ introduced in Eq. (1.4). The operation of pre-multiplying Eq. (3.3) by the matrix in (3.5) can be viewed as one step of Gauss elimination for block matrices and the matrix $\tilde{Q}_2^j$ is often referred to as the *Schur complement*. Note that since the matrix in (3.5) is nonsingular, the matrix $\tilde{Q}_2^j$ is also nonsingular for any basis Ψ^{j-1} of W^{j-1}.

We have thus reduced solving the system in (2.5) to first solving the smaller linear system

$$\tilde{Q}_2^j \boldsymbol{g}^{j-1} = \boldsymbol{f}_2^j - P_2^j \boldsymbol{f}_1^j \tag{3.7}$$

for $\boldsymbol{g}^{j-1}$, and afterwards computing $\boldsymbol{f}^{j-1}$ from the substitution

$$\boldsymbol{f}^{j-1} = \boldsymbol{f}_1^j - Q_1^j \boldsymbol{g}^{j-1}. \tag{3.8}$$

Conversely, in reconstruction, we can compute $\boldsymbol{f}_1^j$ and $\boldsymbol{f}_2^j$, in that order, from $\boldsymbol{f}^{j-1}$ and $\boldsymbol{g}^{j-1}$ using the rearrangements of (3.7)–(3.8),

$$\boldsymbol{f}_1^j = \boldsymbol{f}^{j-1} + Q_1^j \boldsymbol{g}^{j-1}, \tag{3.9}$$

$$\boldsymbol{f}_2^j = P_2^j \boldsymbol{f}_1^j + \tilde{Q}_2^j \boldsymbol{g}^{j-1}. \tag{3.10}$$

Thus the filter bank algorithms A1 and A2 can be replaced by alternative algorithms which use the Schur complement matrix $\tilde{Q}_2^j$ instead of Q_2^j.

Algorithm A1′. Decomposition using the Schur complement.

As Algorithm A1 except that step (i) is replaced by

(i) For each level $j = m, m-1, \ldots, 1$,

(a) solve the linear system (3.7) for $\boldsymbol{g}^{j-1}$ and
(b) compute $\boldsymbol{f}^{j-1}$ from the substitution (3.8).

Algorithm A2′. Reconstruction using the Schur complement.

As Algorithm A2 except that step (i) is replaced by

(i) For each level $j = 1, 2, \ldots, m$,

(a) compute $\boldsymbol{f}_1^j$ from (3.9) and
(b) compute $\boldsymbol{f}_2^j$ from (3.10).

Eq. (3.7) has an interesting geometric interpretation. First recall from (3.1) that the coefficient vector $\boldsymbol{f}^j$ in (2.1) consists of evaluations of f^j, in other words $f_v^j = f^j(v)$ for $v \in V^j$. Combining this observation with (3.4), we deduce that the right-hand side of (3.7) is the column vector whose elements are

$$f^j(u) - (f^j(v_1) + f^j(v_2))/2, \quad u \in V_*^j, \tag{3.11}$$

where v_1 and v_2 are the two coarse level parents of u. This expression can be viewed as the value of $f^j(u)$ relative to the value of the linear interpolant to f^j along the edge $[v_1, v_2]$ at the midpoint u.

4. Prewavelets

In this section we describe a certain choice of complement space W^{j-1} together with a basis Ψ^{j-1}. This will determine Q^j, the remaining matrix in the filter bank algorithms yet to be specified.

Though our main intention is to apply the prewavelet basis constructed in [4], we begin, for the sake of comparison, by discussing the simpler basis appearing in the so-called *Faber decomposition*. This concept dates back, though in a different context, to a paper by Faber [3], and is discussed in a more modern multiresolution setting in [2]. In Faber decomposition one sets

$$\psi_u^{j-1} = \phi_u^j, \quad u \in V_*^j$$

and so the basis Ψ^{j-1} consists of the level j nodal functions at the 'fine' vertices. In the numerical treatment of partial differential equations, the resulting sequence of bases $\Psi^0, \Psi^1, \ldots$ together with Φ^0 is known as the *hierarchical basis* [14]. Since in this case $q_{wu} = \delta_{wu}$, we find $Q_1^j = 0$ and $Q_2^j = I$ in Eq. (3.3) and therefore $\tilde{Q}_2^j = I$ in Eq. (1.4). So Eqs. (3.7) and (3.8) reduce to

$$\begin{aligned} \boldsymbol{g}^{j-1} &= \boldsymbol{f}_2^j - P_2^j \boldsymbol{f}_1^j, \\ \boldsymbol{f}^{j-1} &= \boldsymbol{f}_1^j, \end{aligned} \tag{4.1}$$

which means that $\boldsymbol{f}^{j-1}$ and $\boldsymbol{g}^{j-1}$ can be computed without the need for solving a linear system. In the light of (3.11), the coefficient vector $\boldsymbol{g}^{j-1}$ now simply represents interpolation errors at edge midpoints which is the basic idea of Faber decomposition.

Though Faber decomposition benefits from bases with minimal support, we would prefer a choice of complement space W^{j-1} which is orthogonal to S^{j-1} with respect to some standard inner product, such as the usual one in $L_2(\Omega)$ or the *weighted* one

$$\langle f,g\rangle_* := \sum_{T\in\mathscr{T}^0} \frac{1}{\mathrm{a}(T)} \int_T f(x)g(x)\,\mathrm{d}x, \quad f,g\in C(\Omega) \tag{4.2}$$

where $\mathrm{a}(T)$ is the area of triangle T. This turns the direct sum in (1.2) into an orthogonal one and it is then usual to call any function in W^{j-1} a *prewavelet*. A simple way to construct a basis of prewavelets for W^{j-1} is to take

$$\psi_u^{j-1} = \phi_u^j - P\phi_u^j, \quad u\in V_*^j,$$

where P: $S^j \to S^{j-1}$ is the least-squares operator with respect to the norm induced by the inner product. The prewavelets ψ_u^{j-1}, however, typically have global support and thus generate a full matrix Q^j.

It was this drawback that motivated the construction in [4] of a basis of prewavelets of *local support*, giving rise to a sparse matrix Q^j. Further properties of these prewavelets were derived in [5,6]. These prewavelets generalize those constructed by Kotyczka and Oswald [9] for infinite three-directional meshes. The only other construction of locally supported prewavelets in this setting that we know of is that due to Stevenson [12], though the supports are somewhat larger (see [4] for some discussion). The approach taken in [4] is to start by defining W^{j-1} to be the orthogonal complement of S^{j-1} in S^j with respect to the weighted inner product in (4.2). As was shown in Lemma 2.1 of [6],

$$\langle f,g\rangle_* = 2^{-2j} \sum_{T\in\mathscr{T}^j} \frac{1}{\mathrm{a}(T)} \int_T f(x)g(x)\,\mathrm{d}x, \quad f,g\in C(\Omega)$$

and the scaling of these integrals means that the prewavelet coefficients turn out to be independent of the areas of the triangles. They depend only on the local topology of $\mathscr{T}^j$.

The starting point for describing the prewavelets of [4] is to define what we mean by a *semi-prewavelet*. Starting with a coarse vertex $v\in V^{j-1}$, we let u be any neighbouring fine vertex, i.e. $u\in V_v^j$. So u is the midpoint of some edge $[v,v^*]$ in E^{j-1}. The following was shown in [6].

Lemma 4.1. *For any $\gamma\in\mathbb{R}$, there is a unique function $\sigma_{v,u}^{j-1}$ in S^j of the form*

$$\sigma_{v,u}^{j-1}(x) = A\phi_v^j(x) + \sum_{w\in V_v^j} B_w\phi_w^j(x) \tag{4.3}$$

such that for any coarse vertex $a\in V^{j-1}$,

$$\langle \phi_a^{j-1}, \sigma_{v,u}^{j-1}\rangle_* = \begin{cases} -2^{-2j}\gamma & \text{if } a=v,\\ 2^{-2j}\gamma & \text{if } a=v^*,\\ 0 & \text{otherwise.}\end{cases}$$

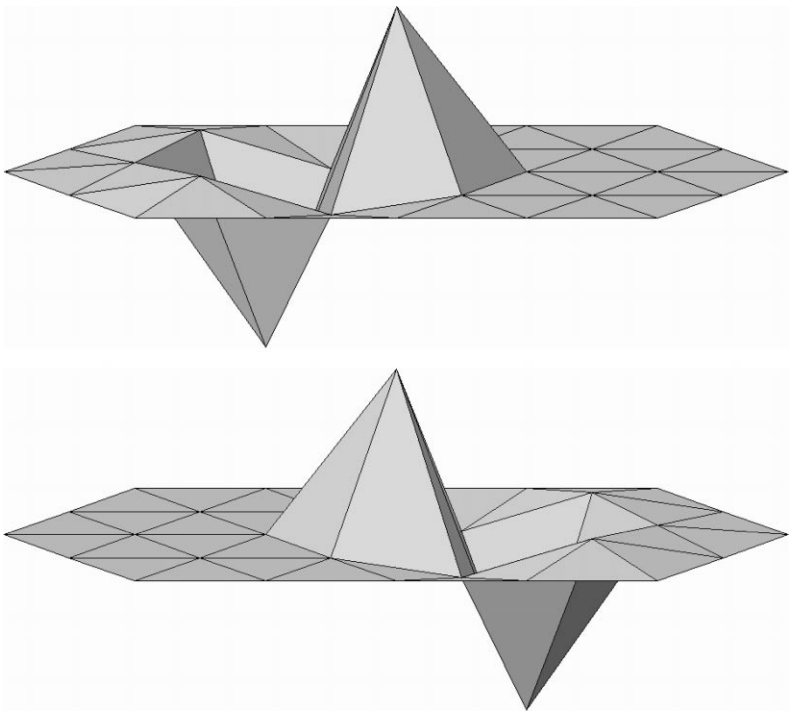

Fig. 1. A pair of semi-prewavelets associated with an interior vertex.

We call $\sigma_{v,u}^{j-1}$ (when $\gamma \neq 0$) a `semi-prewavelet` for the simple reason that the function

$$\psi_u^{j-1} = \sigma_{v,u}^{j-1} + \sigma_{v^*,u}^{j-1}$$

is orthogonal to all basis functions in S^{j-1} and is consequently a prewavelet as illustrated in Figs. 1 and 2. Since the support of $\sigma_{v,u}^{j-1}$ is by definition contained in M_v^{j-1}, the support of ψ_u^{j-1} is contained in $M_v^{j-1} \cup M_{v^*}^{j-1}$.

It was shown in Theorem 4.1 of [6] that the prewavelets ψ_u^{j-1} form a basis of W^{j-1} and in Theorem 5.1 of [6] that they are also *stable* in the sense that there exist constants $C_1, C_2 > 0$, independent of j, such that for all sequences $\{d_u\}_{u \in V_*^j}$,

$$C_1 \sum_{u \in V_*^j} d_u^2 \leqslant \left\| \sum_{u \in V_*^j} d_u 2^{j-1} \psi_u^{j-1}(\cdot) \right\|_*^2 \leqslant C_2 \sum_{u \in V_*^j} d_u^2,$$

where $\|.\|_*$ denotes the norm induced by the weighted inner product of (4.2).

In Lemma 3.4 of [6], the following useful symmetry properties were shown, namely that for any coarse $v \in V^{j-1}$ and any two of its fine neighbours $u, w \in V_v^j$,

$$\sigma_{v,u}^{j-1}(w) = \sigma_{v,w}^{j-1}(u), \tag{4.4}$$

which implies that for any $u, w \in V_*^j$,

$$\psi_u^{j-1}(w) = \psi_w^{j-1}(u). \tag{4.5}$$

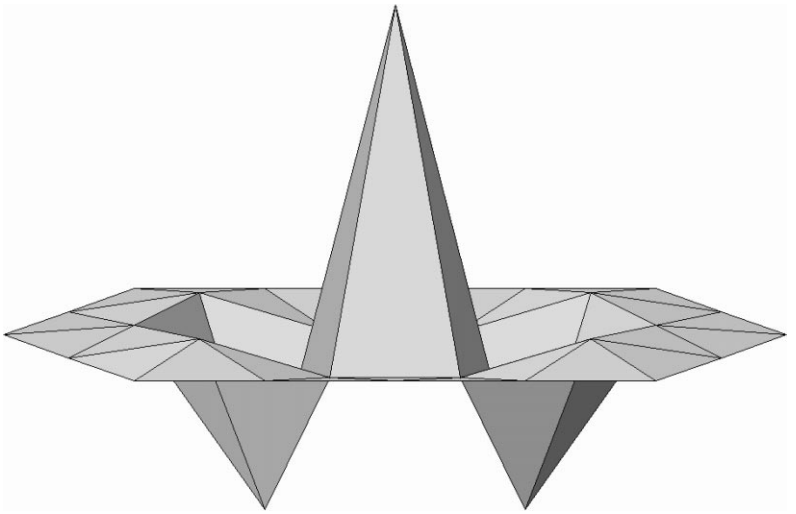

Fig. 2. A prewavelet as the sum of the two semi-prewavelets in Fig. 1.

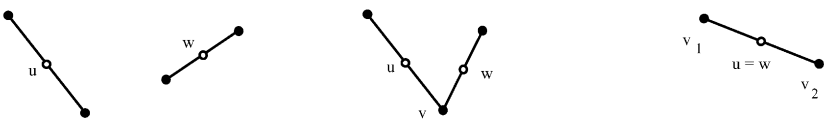

(a) $N_{wu}^{j-1} = \emptyset$ (b) $N_{wu}^{j-1} = \{v\}$ (c) $N_{wu}^{j-1} = \{v_1, v_2\}$

Fig. 3. Three cardinalities of the set N_{wu}^{j-1}.

From the supports and symmetry properties of the prewavelets we deduce the structure of the (sparse) matrices Q_1^j and Q_2^j in the two-scale matrix (3.3). The $|V^{j-1}| \times |V_*^j|$ submatrix Q_1^j of Q^j has entries

$$q_{vu} = \begin{cases} \sigma_{v,u}^{j-1}(v) & \text{if } u \in V_v^j, \\ 0 & \text{otherwise,} \end{cases} \tag{4.6}$$

for $v \in V^{j-1}$ and $u \in V_*^j$. This means that the column of Q_1^j associated with the fine vertex u has precisely two nonzero entries, namely in the rows associated with its two coarse level parents. Conversely, the row v of Q_1^j has $|V_v^j|$ nonzero entries. Note also that according to (3.4), the sparsity patterns of Q_1^j and $(P_2^j)^{\mathrm{T}}$ are identical.

Meanwhile, in order to describe the structure of the square submatrix Q_2^j of dimension $|V_*^j|$, let N_{wu}^{j-1} denote the set of common coarse neighbours of two fine vertices w and u, i.e.

$$N_{wu}^{j-1} = N_{uw}^{j-1} = \{v \in V^{j-1} : u, w \in V_v^j\}, \quad u, w \in V_*^j.$$

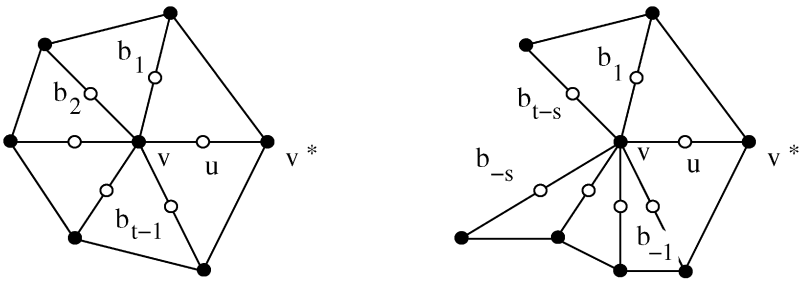

Fig. 4. The sets M_v^{j-1} for (a) an interior and (b) a boundary vertex v.

Clearly, the cardinality of N_{wu}^{j-1} is always either 0, 1 or 2 as illustrated in Fig. 3. Then, by taking into account the supports of the semi-prewavelets, we can express the elements of Q_2^j as

$$q_{wu} = \sum_{v \in N_{wu}^{j-1}} \sigma_{v,u}^{j-1}(w), \quad u, w \in V_*^j, \tag{4.7}$$

where we use the standard convention that the sum is zero when $N_{wu}^{j-1} = \emptyset$. From this expression and (4.4), we see that Q_2^j is symmetric and, moreover, the column given by u has at most $|V_{v_1}^j| + |V_{v_2}^j| - 1$ nonzero elements, where v_1 and v_2 are the coarse level neighbours of u.

Let us now turn to explicit expressions for the semi-prewavelet coefficients (and by implication the prewavelet coefficients), namely A and B_w for $w \in V_v^j$ in (4.3), which are independent of j. As in [6], we let $\gamma = \frac{1}{6}$ in Lemma 4.1. We then define the constant

$$\lambda = (-5 + \sqrt{21})/2,$$

which is a solution of the homogeneous equations

$$\lambda^{k-1} + 5\lambda^k + \lambda^{k+1} = 0, \quad k \in \mathbb{Z}. \tag{4.8}$$

Then we specify the semi-prewavelet coefficients in the two distinct cases (1) v is an interior vertex and (2) v is a boundary vertex; see Fig. 4. In both cases, let $t(v)$ denote the number of triangles in $\mathscr{T}^{j-1}$ (or $\mathscr{T}^j$) incident on v.

We begin with an interior vertex v, where $t(v) = |V_v^j| \geqslant 3$, and we denote the neighbours of v in $\mathscr{T}^j$ anticlockwise, by b_i, $i = 0, \ldots, t(v) - 1$, with $b_0 = u$, as in Fig. 4a. It was shown in [6] that

$$\sigma_{v,u}^{j-1}(v) = -\frac{3}{2t(v)} \quad \text{and} \quad \sigma_{v,u}^{j-1}(b_i) = \frac{3}{28t(v)} + \theta(i, t(v)), \quad i = 0, 1, \ldots, t(v) - 1, \tag{4.9}$$

where

$$\theta(i,t) := \frac{\lambda^i + \lambda^{t-i}}{\sqrt{21}(1 - \lambda^t)}.$$

Alternatively, suppose that v is a boundary vertex, where $t(v) = |V_v^j| - 1 \geqslant 1$, and order its neighbours in $\mathscr{T}^j$ as in Fig. 4b. Let $s \geqslant 0$ be the number of triangles in M_v^j counting clockwise from the oriented edge $[v, v^*]$ in E^{j-1} containing u. The neighbouring vertices of v in anticlockwise order can then be

denoted b_i, $i=-s,\dots,t(v)-s$, so that $b_0=u$. It was shown in [6] that

$$\sigma_{v,u}^{j-1}(v)=-\frac{3}{2t(v)} \quad \text{and} \quad \sigma_{v,u}^{j-1}(b_i)=\frac{3}{28t(v)}+\theta(i,s,t(v)),\ \ i=-s,\dots,t(v)-s, \tag{4.10}$$

where

$$\theta(i,s,t):=\begin{cases}\dfrac{(\lambda^{t-s}+\lambda^{-t+s})(\lambda^{s+i}+\lambda^{-s-i})}{\sqrt{21}(\lambda^{-t}-\lambda^{t})}, & i=-s,\dots,0,\\ \dfrac{(\lambda^{s}+\lambda^{-s})(\lambda^{t-s-i}+\lambda^{-t+s+i})}{\sqrt{21}(\lambda^{-t}-\lambda^{t})}, & i=1,\dots,t-s.\end{cases}$$

In order to analyse the properties of the Schur complement matrix $\tilde{Q}_2^j$ in the subsequent section, it is advantageous to gather in a matrix all the values of θ associated with any coarse vertex $v\in V^{j-1}$.

Recall first that it is usual to denote a circulant matrix M by $\mathrm{circ}(m_1,m_2,\dots,m_\ell)$ (see [1]), meaning that M is a square matrix of size ℓ with $(m_1,m_2,\dots,m_\ell)$ as its first row and with the entries of the i-th row obtained by rotating right the first row $i-1$ times, i.e. $m_{ik}=m_{k-i+1 \bmod \ell}$.

For a given coarse vertex $v\in V^{j-1}$, we now define the matrix Θ_v to be a square matrix of size $|V_v^j|$, which is equal to $t(v)$ if v is in the interior and $t(v)+1$ if v is on the boundary. Letting $t=t(v)$, we set for an interior vertex v,

$$\Theta_v=(\theta((k-i) \bmod t,t))_{i,k=1,t}=\mathrm{circ}(\theta(0,t),\dots,\theta(t-1,t)) \tag{4.11}$$

and for a boundary vertex v,

$$\Theta_v=(\theta(i,k,t))_{i,k=0,t}. \tag{4.12}$$

Note that the matrix Θ_v only depends on $t(v)$ and whether v is an interior or boundary vertex of $\mathscr{T}^{j-1}$. It was shown in [6] that Θ_v is symmetric.

In [6], the linear independence of the prewavelets ψ_u^{j-1} was established by deriving the positive definiteness of the matrix Q_2^j in (3.3) from the positive definiteness of the matrices Θ_v for all $v\in V^{j-1}$. We remark that the following new results, in addition to being useful for the analysis of the Schur complement matrix $\tilde{Q}_2^j$ in Section 5, provide a straightforward way to establish the positive definiteness of Θ_v instead of invoking the more involved estimates on the functions θ used in [6].

By direct computation using (4.11), (4.12) and the relation (4.8), we obtain the following.

Lemma 4.2. *The matrix Θ_v is invertible and its inverse A_v is*

$$\begin{pmatrix}5&1&0&\cdots&0&0&1\\1&5&1&\cdots&0&0&0\\\vdots&\vdots&\vdots&\dots&\vdots&\vdots&\vdots\\0&0&0&\cdots&1&5&1\\1&0&0&\cdots&0&1&5\end{pmatrix} \quad \textit{or} \quad \begin{pmatrix}\frac{5}{2}&1&0&\cdots&0&0&0\\1&5&1&\cdots&0&0&0\\\vdots&\vdots&\vdots&\dots&\vdots&\vdots&\vdots\\0&0&0&\cdots&1&5&1\\0&0&0&\cdots&0&1&\frac{5}{2}\end{pmatrix},$$

depending on whether v is an interior or boundary vertex respectively.

Thus the inverse of Θ_v has a very simple structure, namely $A_v=\mathrm{circ}(5,1,0,\dots,0,1)$ in the interior case, with only slight modifications in the corners for the boundary case.

Denoting by $\lambda(M)$ the set of all eigenvalues of a matrix M, we obtain immediately from Gershgorin's circle theorem that

$$\tfrac{3}{2} \leqslant \lambda(A_v) \leqslant 7$$

and consequently we have

Corollary 4.3. *For any $v \in V^{j-1}$, the symmetric matrix Θ_v is positive definite and its eigenvalues satisfy the inequalities*

$$\tfrac{1}{7} \leqslant \lambda(\Theta_v) \leqslant \tfrac{2}{3}.$$

As can be seen from (4.9) and (4.10), the elements of Θ_v constitute the main ingredients of the semi-prewavelet coefficients at fine vertices associated with the coarse vertex $v \in V^{j-1}$. Indeed, let Q_v be the $|V_v^j| \times |V_v^j|$ matrix

$$Q_v = (q_{vwu})_{w,u \in V_v^j} = (\sigma_{v,u}^{j-1}(w))_{w,u \in V_v^j}, \tag{4.13}$$

with rows and columns ordered as in Θ_v. Then if we let $\mathbf{1}_v$ be the $|V_v^j| \times |V_v^j|$ matrix with all elements equal to 1, we have from (4.9) and (4.10) that

$$Q_v = \frac{3}{28t(v)}\mathbf{1}_v + \Theta_v. \tag{4.14}$$

For example, when v is an interior vertex with 6 incident triangles,

$$\Theta_v = \tfrac{1}{504}\mathrm{circ}(110, -23, 5, -2, 5, -23),$$

$$Q_v = \tfrac{1}{72}\mathrm{circ}(17, -2, 2, 1, 2, -2).$$

If v is a boundary vertex with 3 incident triangles we have

$$\Theta_v = \frac{1}{504}\begin{pmatrix} 220 & -46 & 10 & -4 \\ -46 & 115 & -25 & 10 \\ 10 & -25 & 115 & -46 \\ -4 & 10 & -46 & 220 \end{pmatrix} \quad \text{and} \quad Q_v = \frac{1}{72}\begin{pmatrix} 34 & -4 & 4 & 2 \\ -4 & 19 & -1 & 4 \\ 4 & -1 & 19 & -4 \\ 2 & 4 & -4 & 34 \end{pmatrix}.$$

5. Properties of the Schur complement matrix

We observed in Section 3 that the Schur complement matrix is non-singular. In this section we show that, unlike the original two scale matrix in (2.5), it is also symmetric and positive definite. Moreover we derive some bounds on its eigenvalues and show that it has a small condition number.

First we establish some basic facts about the Schur complement matrix.

Proposition 5.1. *The Schur complement matrix $\tilde{Q}_2^j$ in* (1.4) *is symmetric and its elements are*

$$\tilde{q}_{wu} = \sum_{v \in N_{wu}^{j-1}} \left(\sigma_{v,u}^{j-1}(w) + \frac{3}{4t(v)}\right), \quad u, w \in V_*^j. \tag{5.1}$$

Proof. From the elements of the matrices P_2^j and Q_1^j given in equations (3.4) and (4.6), and recalling the value of a semi-prewavelet at a coarse vertex in equations (4.9) and (4.10), we find that the elements of the matrix $D:=P_2^jQ_1^j$ are

$$d_{wu}=\sum_{v\in V^{j-1}}p_{wv}q_{vu}=\sum_{v\in N_{wu}^{j-1}}\frac{1}{2}\sigma_{v,u}^{j-1}(v)=-\sum_{v\in N_{wu}^{j-1}}\frac{3}{4t(v)},$$

for $w,u\in V_*^j$. Since, by definition (1.4), $\tilde{q}_{wu}=q_{wu}-d_{wu}$, this yields Eq. (5.1). That $\tilde{q}_{wu}=\tilde{q}_{uw}$ is immediate from the semi-prewavelet symmetry expressed in (4.4). □

We note that $\tilde{Q}_2^j$ is sparse and we see from (5.1) that, similar to Q_2^j, its elements satisfy $\tilde{q}_{wu}=0$ whenever $N_{wu}^{j-1}=\emptyset$. We next bound the eigenvalues of $\tilde{Q}_2^j$.

Theorem 5.2. *The eigenvalues of the Schur complement $\tilde{Q}_2^j$ are bounded independently of j as*

$$\tfrac{2}{7}\leqslant\lambda(\tilde{Q}_2^j)\leqslant\tfrac{100}{21}.$$

We will prove this assertion by means of the symmetric square matrices

$$\tilde{Q}_v=(\tilde{q}_{vwu})_{w,u\in V_v^j},\quad v\in V^{j-1} \tag{5.2}$$

of dimension $|V_v^j|$, with the same ordering as for Θ_v and Q_v in (4.11–4.13), and where

$$\tilde{q}_{vwu}=\sigma_{v,u}^{j-1}(w)+\frac{3}{4t(v)},\quad u,w\in V_v^j.$$

Thus, in the two examples of Section 4, we have for an interior vertex v with six incident edges,

$$\tilde{Q}_v=\tilde{Q}_{6,i}:=\tfrac{1}{72}\mathrm{circ}(26,7,11,10,11,7) \tag{5.3}$$

and for a boundary vertex v with 4 incident edges,

$$\tilde{Q}_v=\tilde{Q}_{4,b}:=\frac{1}{72}\begin{pmatrix}52&14&22&20\\14&37&17&22\\22&17&37&14\\20&22&14&52\end{pmatrix}. \tag{5.4}$$

We first show that the eigenvalues of the global matrix $\tilde{Q}_2^j$ are sandwiched by the minimum and maximum eigenvalues of the local matrices $\tilde{Q}_v$.

Lemma 5.3. *The eigenvalues of $\tilde{Q}_2^j$ are bounded as*

$$2\min_{v\in V^{j-1}}\lambda_{\min}(\tilde{Q}_v)\leqslant\lambda(\tilde{Q}_2^j)\leqslant 2\max_{v\in V^{j-1}}\lambda_{\max}(\tilde{Q}_v).$$

Proof. Recall that the minimum and maximum eigenvalues of a symmetric matrix A can be expressed as the Rayleigh quotients

$$\lambda_{\min}(A)=\min_{x\neq 0}\frac{x^{\mathrm{T}}Ax}{x^{\mathrm{T}}x}\quad\text{and}\quad\lambda_{\max}(A)=\max_{x\neq 0}\frac{x^{\mathrm{T}}Ax}{x^{\mathrm{T}}x}.$$

Therefore let $\boldsymbol{x} = (x_w)_{w \in V_*^j}$ be any vector of real numbers not all equal to zero. Then

$$\begin{aligned}\sum_{u,w \in V_*^j} x_u x_w \tilde{q}_{uw} &= \sum_{v \in V^{j-1}} \sum_{u,w \in V_v^j} x_u x_w \tilde{q}_{vuw} \\ &\geqslant \sum_{v \in V^{j-1}} \lambda_{\min}(\tilde{Q}_v) \sum_{u \in V_v^j} x_u^2 \\ &\geqslant \left(\min_{v \in V^{j-1}} \lambda_{\min}(\tilde{Q}_v) \right) \sum_{v \in V^{j-1}} \sum_{u \in V_v^j} x_u^2 \\ &= 2 \min_{v \in V^{j-1}} \lambda_{\min}(\tilde{Q}_v) \sum_{u \in V_*^j} x_u^2,\end{aligned}$$

and since this inequality holds for all nonzero $\boldsymbol{x}$, it follows that any eigenvalue of $\tilde{Q}_2^j$ satisfies

$$\lambda(\tilde{Q}_2^j) \geqslant 2 \min_{v \in V^{j-1}} \lambda_{\min}(\tilde{Q}_v).$$

An analogous argument establishes the upper bound. □

In order to prove Theorem 5.2 it thus remains to bound the eigenvalues of the local matrices $\tilde{Q}_v$ as follows.

Lemma 5.4. *The eigenvalues of the matrices $\tilde{Q}_v$ are bounded independently of the vertex v as* $\frac{1}{7} \leqslant \lambda(\tilde{Q}_v) \leqslant \frac{50}{21}$.

Proof. From (5.2) and (4.14) we have

$$\tilde{Q}_v = \frac{3}{4t(v)} \mathbf{1}_v + Q_v = \frac{6}{7t(v)} \mathbf{1}_v + \Theta_v.$$

The eigenvalues of the matrix $\mathbf{1}_v$ are 0 and $|V_v^j|$ and since $|V_v^j| = t(v)$ for interior vertices and $|V_v^j| = t(v)+1$ for boundary vertices, we find that the eigenvalues of $(6/7t(v))\mathbf{1}_v$ are bounded uniformly by 0 and 12/7. Combining these estimates with those for the eigenvalues of Θ_v in Corollary 4.3, establishes the result, using the fact that the eigenvalues of the sum of two matrices are bounded from below and above by the sums of the smallest and largest eigenvalues, respectively. □

The combination of Lemmas 5.3 and 5.4 now yields Theorem 5.2, which in turn leads to the following corollary.

Corollary 5.5. *The Schur complement matrix $\tilde{Q}_2^j$ is symmetric, positive definite, and uniformly conditioned with condition number*

$$\kappa(\tilde{Q}_2^j) = \frac{\lambda_{\max}(\tilde{Q}_2^j)}{\lambda_{\min}(\tilde{Q}_2^j)} \leqslant \frac{50}{3}.$$

We complete this section by discussing how the Schur complement can be treated in Algorithms A1′ and A2′. In general, the inverse of the sparse Schur complement $\tilde{Q}_2^j$ is a full matrix. Additionally,

the nonzero elements of $\tilde{Q}_2^j$ do not usually form a uniform sparsity pattern such as a band, as is often the case in univariate and tensor-product bivariate spline problems. Consequently, neither the actual computation of $(\tilde{Q}_2^j)^{-1}$ nor the use of a general sparse solver with unavoidable fill-in are suitable for an efficient implementation. Instead, the properties of $\tilde{Q}_2^j$ established in Corollary 5.5 clearly indicate that it is better to solve the linear system (3.7) iteratively. In our numerical examples we have employed the conjugate gradient (CG) method, see [8].

In order to apply the CG method, it is not necessary to set up the (global) matrix $\tilde{Q}_2^j$ explicitly. We can perform iterations in-place, using the local matrices $\tilde{Q}_v$, thereby minimizing memory requirements. Specifically, in the CG method we only need to perform a matrix-vector multiplication of the form

$$\boldsymbol{r}:=\tilde{Q}_2^j\boldsymbol{x}$$

for a given vector $\boldsymbol{x}=(x_u)_{u\in V_*^j}$. Let $\boldsymbol{x}_v=(x_u)_{u\in V_v^j}$ be the vector of length $|V_v^j|$ containing only those (local) components of the (global) vector $\boldsymbol{x}$ which correspond to fine neighbours of a given coarse vertex $v\in V^{j-1}$. By Proposition 5.1, we see that for a given fine vertex $w\in V_*^j$ with coarse level parents v_1 and v_2, we can compute the component r_w from the local matrices $\tilde{Q}_{v_1}$ and $\tilde{Q}_{v_2}$ because

$$r_w=\sum_{u\in V_*^j}\tilde{q}_{wu}x_u=\sum_{u\in V_{v_1}^j}\tilde{q}_{v_1wu}x_u+\sum_{u\in V_{v_2}^j}\tilde{q}_{v_2wu}x_u=(\tilde{Q}_{v_1}\boldsymbol{x}_{v_1})_w+(\tilde{Q}_{v_2}\boldsymbol{x}_{v_2})_w.$$

Starting with $\boldsymbol{r}=\boldsymbol{0}$, we can thus perform the matrix-vector multiplication by iterating over the vertices v in V^{j-1}, and updating for each $w\in V_v^j$ by $r_w:=r_w+\tilde{q}_{vwu}x_u$ for all $u\in V_v^j$.

Finally, very few of all the matrices $\tilde{Q}_v$, $v\in V^{m-1}$, used in Algorithms A1′ or A2′ are distinct. To see this we first note that $\tilde{Q}_v$ depends only on whether v is an interior or boundary vertex and the number of incident edges, degree $d(v)$. Therefore, since the degree of a vertex is invariant under refinement, and the degree of a vertex v not in V^0 is either $d(v)=6$ if v is an interior vertex, or $d(v)=4$ if v is a boundary vertex, all matrices $\tilde{Q}_v$, for $v\in V^{m-1}$, are contained in

$$\{\tilde{Q}_v : v\in V^0\}\cup\{\tilde{Q}_{6,i},\tilde{Q}_{4,b}\},$$

where $\tilde{Q}_{6,i}$ and $\tilde{Q}_{4,b}$ are defined in (5.3) and (5.4). Moreover, this set will be typically quite small, since several of the matrices $\tilde{Q}_v$, for $v\in V^0$ will be repeated. For example amongst the 99 vertices of V^0 in Fig. 8a, the number of distinct matrices is 12, and there are no new ones for V^1 (in Fig. 8b).

6. Numerical examples

We complete the paper with two numerical examples. They compare Faber and prewavelet decomposition with respect to thresholding as explained at the end of Section 2. In addition we compute the condition numbers of the Schur complements for prewavelet decomposition.

In our examples we decompose a given function f^m in S^m and perform thresholding and reconstruction, yielding an approximation with error e^m given by Eq. (2.7). We measure this error in

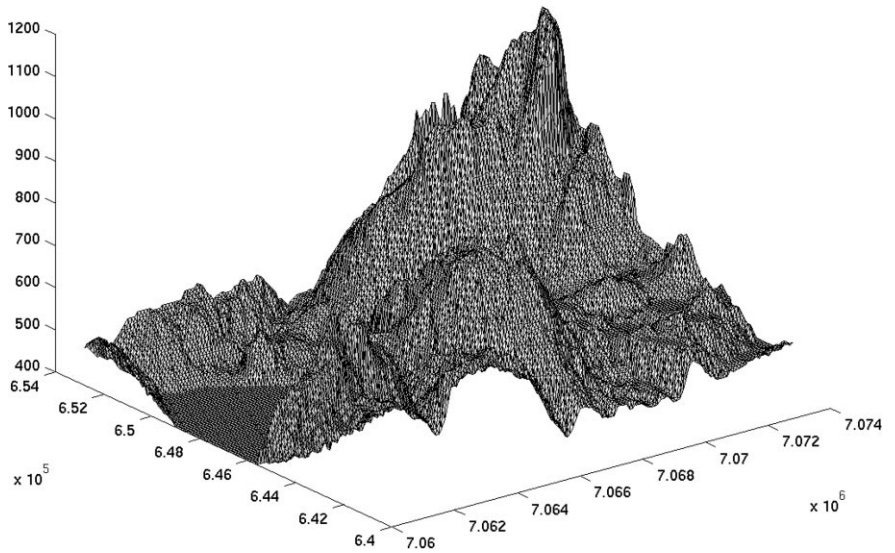

Fig. 5. Terrain model.

several ways: the weighted L_2 norm defined in (4.2) which reduces to

$$\|e^m\|_*^2 = \frac{2^{-2m}}{6} \sum_{T=[w_1,w_2,w_3]\in\mathscr{T}^m} (e_1^2 + e_2^2 + e_3^2 + e_1e_2 + e_2e_3 + e_3e_1),$$

where $e_i = e^m(w_i)$; the maximum error given by

$$\|e^m\|_\infty = \max_{x\in\Omega} |e^m(x)| = \max_{v\in V^m} |e^m(v)|$$

and the mean absolute error over the vertices,

$$\text{mean}(e^m) = \frac{1}{|V^m|} \sum_{v\in V^m} |e^m(v)|.$$

Note that for a uniform triangulation, the weighted L_2 norm can be viewed as the usual L_2 norm as it differs only by a scaling. For a nonuniform triangulation we are also interested in the usual L_2 norm given by

$$\|e^m\|^2 = \int_\Omega e^m(x)^2 \,\mathrm{d}x = \frac{1}{6} \sum_{T=[w_1,w_2,w_3]\in\mathscr{T}^m} a(T)(e_1^2 + e_2^2 + e_3^2 + e_1e_2 + e_2e_3 + e_3e_1).$$

The first example is that of a Norwegian terrain model in the form of a $129 \times 129 = 16641$ rectangular grid of points (x, y, z), whose z values represent heights above sea level. The grid was viewed as a type-I triangulation $\mathscr{T}^7$ by adding a diagonal edge to each rectangle and thus the data can be regarded as a piecewise linear function f^7 in S^7; shown in Fig. 5. This function was then decomposed into f^0 and $g^0, \ldots, g^6$ by first using the Faber scheme and secondly by the prewavelet scheme. Since $\dim(S^0)$=4, the coarse function f^0 has just 4 nodal coefficients and the detail functions $g^0, \ldots, g^6$ have between them 16637 coefficients. The detail coefficients were then thresholded to give

Table 1
Error in Faber approximation

Comp. rate	Weighted L_2	Max error	Mean abs. error
0	214.75	468.05	124.23
0.01	34.35	85.00	20.09
0.05	15.43	44.13	8.91
0.1	10.07	31.75	5.96
0.5	1.32	9.19	0.58

Table 2
Error in Prewavelet approximation

Comp. rate	Weighted L_2	Max error	Mean abs. error
0	146.36	433.05	78.83
0.01	21.23	113.94	12.22
0.05	8.35	63.67	5.55
0.1	5.64	35.10	4.12
0.5	1.27	10.17	1.03

Table 3
Condition numbers and CG iterations.

Level j	Matrix size	$\kappa(\tilde{Q}_2^j)$	Iterations
7	12 416	8.887	19
6	3 136	8.873	19
5	800	8.822	19
4	208	8.630	18
3	56	7.994	17
2	16	6.643	13
1	5	3.314	5

specific compression rates and the approximations constructed. The resulting approximation error e^7 given by equation (2.7) is shown in Tables 1 and 2 in the Faber and prewavelet cases, respectively.

Fig. 6 shows the decompositions f^4, f^3, and f^2 of f^7 with respect to the Faber scheme (on the left) and prewavelets (on the right). Fig. 7 shows the respective approximations tabulated in Tables 1 and 2 for compression rates of 1 and 5%.

The uniform conditioning of the Schur complement matrices was confirmed by our numerical experiments. In Table 3 we have calculated the spectral condition numbers and the number of Conjugate Gradient iterations for the Schur complement matrix at each level of decomposition. We used the l_2 norm of the residual as the stop criterion with tolerance $\varepsilon = 10^{-6}$. We see that the condition numbers are roughly constant and typically around half the estimate in Corollary 5.5 (for the highest levels). As one might expect from this, we see from the table that the number of iterations is also roughly constant for the highest levels.

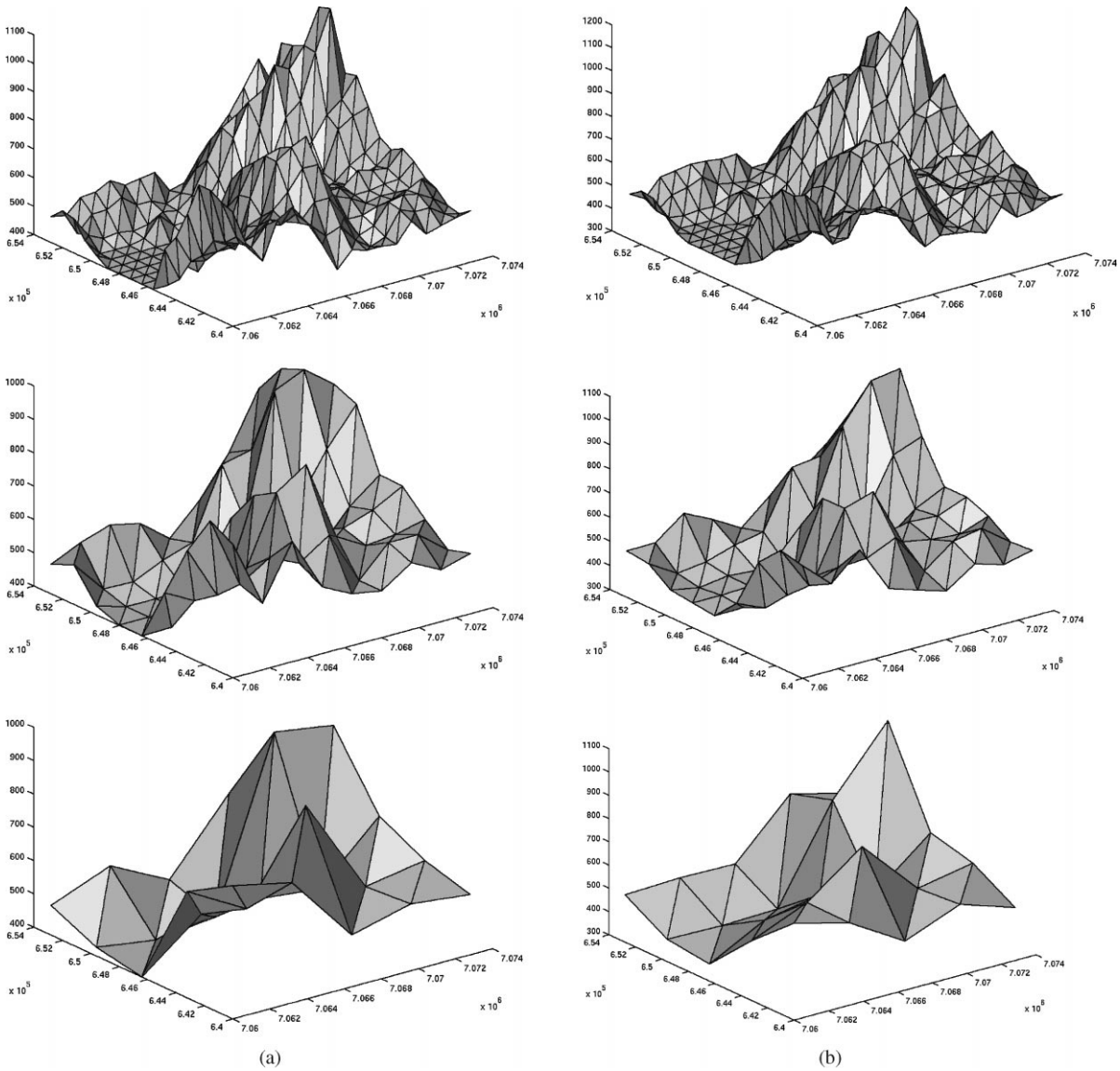

Fig. 6. Levels of decomposition w.r.t. (a) Faber and (b) prewavelets.

In the second example we took a set of 99 points in the plane and generated from them a Delaunay triangulation $\mathscr{T}^0$ shown in Fig. 8a. This was then refined to yield $\mathscr{T}^1$, shown in Fig. 8b, and so on until $\mathscr{T}^4$ was reached. Then the Franke function [7] was sampled at the vertices in V^4, yielding the piecewise linear function f^4. Fig. 9 shows f^4 and Fig. 10 the prewavelet approximation $\hat{f}^4$ using a compression rate of 1%.

Tables 4 and 5 show the approximation error of the Faber and prewavelet schemes, respectively, and Table 6 the Schur complement condition numbers and number of CG iterations. Though we found

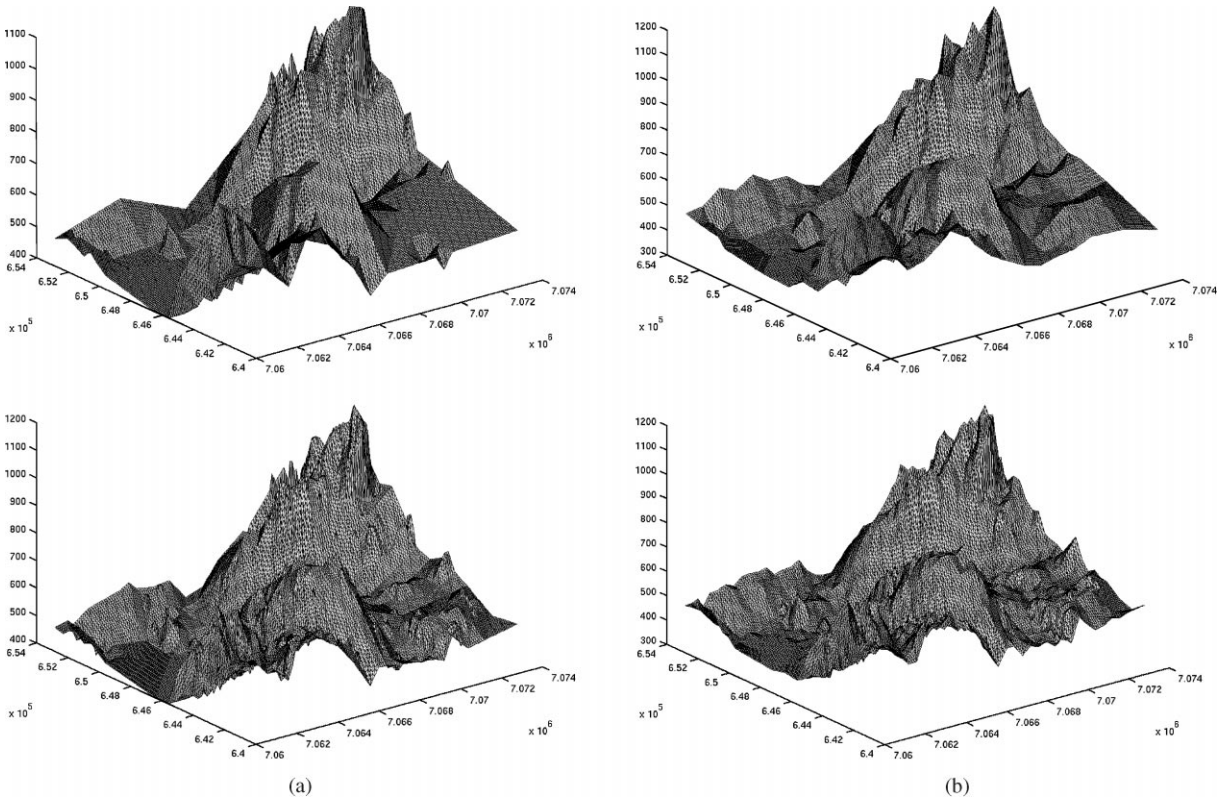

Fig. 7. Approximations w.r.t. (a) Faber and (b) prewavelets.

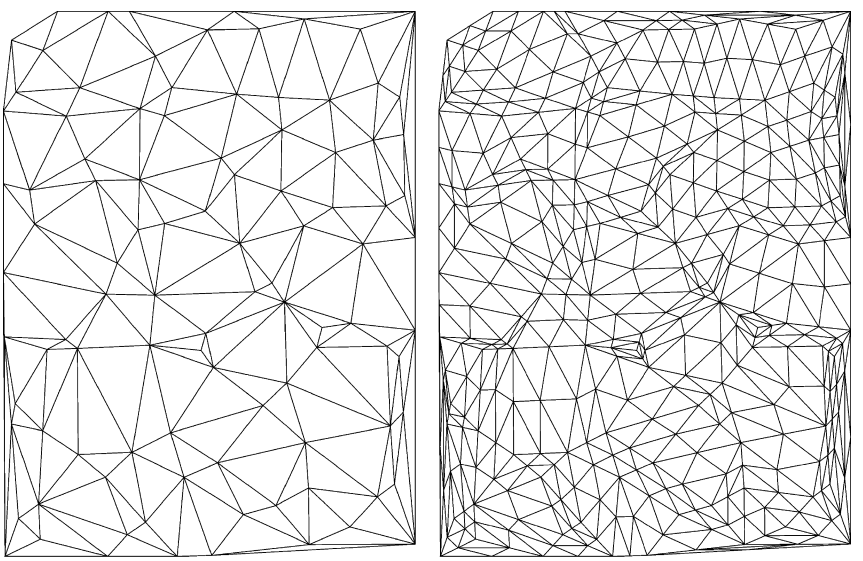

Fig. 8. (a) The triangulation $\mathscr{T}^0$ and (b) its refinement $\mathscr{T}^1$.

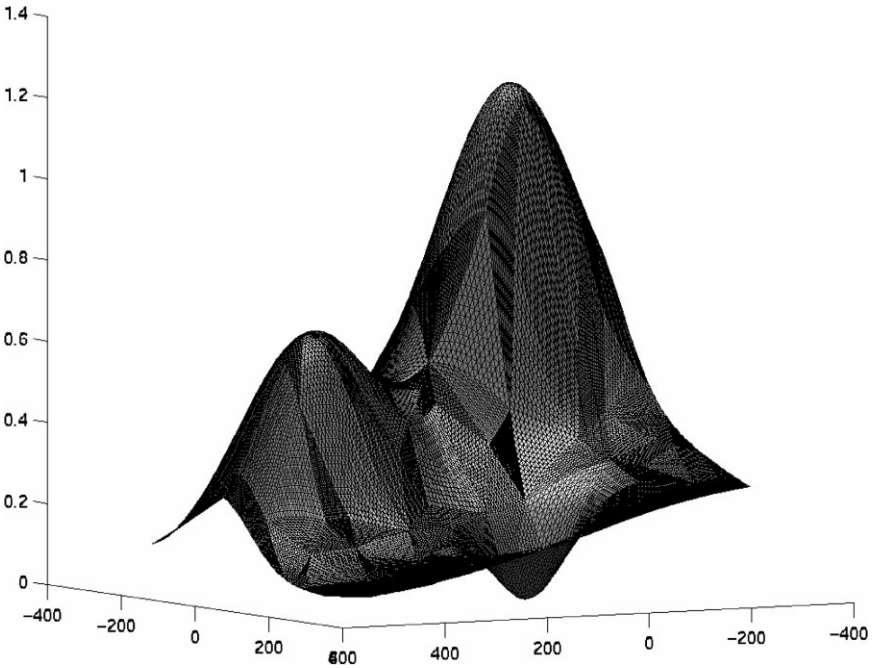

Fig. 9. Piecewise linear approximation of the Franke function f^4.

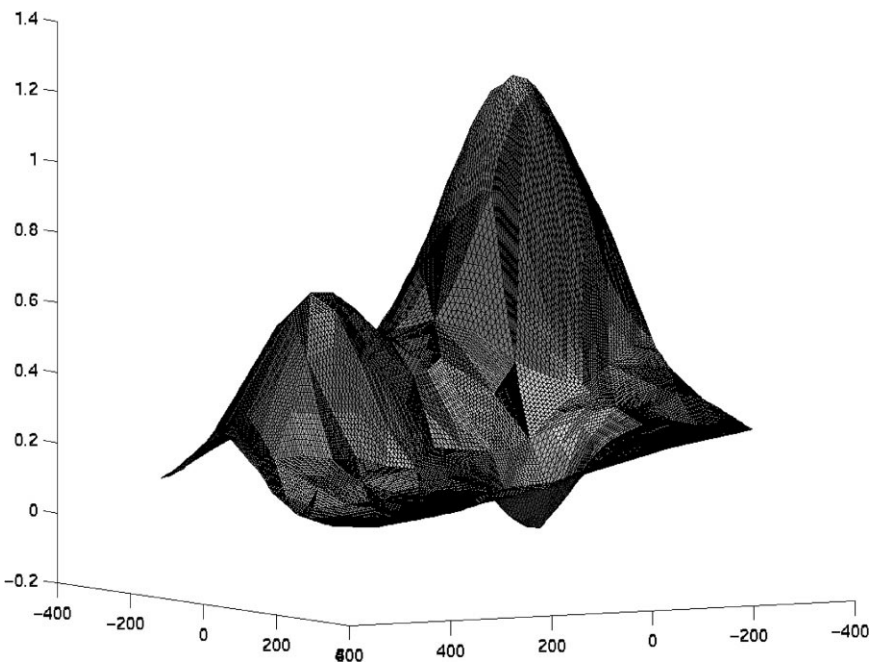

Fig. 10. Prewavelet approximation $\tilde{f}^4$, 1% compression rate.

Table 4
Error in Faber approximation

Comp. rate	L_2	Weighted L_2	Max error	Mean abs. error
0	18.859357	0.316439	0.201259	0.012150
0.01	2.691939	0.054231	0.015546	0.003094
0.05	0.660468	0.013695	0.004123	0.000844
0.1	0.325628	0.006923	0.002042	0.000439
0.5	0.027928	0.000626	0.000243	0.000036

Table 5
Error in prewavelet approximation

Comp. rate	L_2	Weighted L_2	Max error	Mean abs. error
0	11.470842	0.213057	0.156613	0.009235
0.01	1.658807	0.032366	0.017209	0.001899
0.05	0.348691	0.006691	0.004641	0.000445
0.1	0.172943	0.003304	0.003059	0.000246
0.5	0.018938	0.000404	0.000298	0.000034

Table 6
Condition numbers and CG iterations

Level j	Matrix size	$\kappa(\tilde{Q}_2^j)$	Iterations
4	17344	7.69	14
3	4352	7.67	15
2	1096	7.59	17
1	278	7.33	17

little visible difference in $\hat{f}^4$ between the prewavelet and Faber schemes, Tables 4 and 5 reveal that the prewavelet error is typically about half the Faber error w.r.t. both the L_2 and weighted L_2 norms.

References

[1] P.J. Davis, Circulant Matrices, Wiley, New York, 1979.
[2] M.T. Dæhlen, T. Lyche, K. Mørken, H.-P. Seidel, Multiresolution analysis based on quadratic Hermite interpolation – Part 1: Piecewise polynomial curves, preprint.
[3] G. Faber, Über stetige Funktionen, Math. Ann. 66 (1909) 81–94.
[4] M.S. Floater, E.G. Quak, Piecewise linear prewavelets on arbitrary triangulations, Numer. Math. 82 (1999) 221–252.
[5] M.S. Floater, E.G. Quak, A semi-prewavelet approach to piecewise linear prewavelets on triangulations, in: C.K. Chui, L.L. Schumaker (Eds.), Approximation Theory IX, Vol 2, Computational Aspects, Vanderbilt University Press, Nashville, 1998, pp. 63–70.
[6] M.S. Floater, E.G. Quak, Linear independence and stability of piecewise linear prewavelets on arbitrary triangulations, SIAM J. Numer. Anal., to appear.
[7] R. Franke, Scattered data interpolation: test of some methods, Math. Comput. 38 (1982) 181–200.

[8] M.R. Hestenes, E. Stiefel, Methods of conjugate gradients for solving linear systems, Nat. Bur. Standards J. Res. 49 (1952) 409–436.
[9] U. Kotyczka, P. Oswald, Piecewise linear prewavelets of small support, in: C.K. Chui, L.L. Schumaker (Eds.), Approximation Theory VIII, Vol. 2, World Scientific, Singapore, 1995, pp. 235–242.
[10] M.J. Lai, L.L. Schumaker, Splines on Triangulations, to appear.
[11] P. Oswald, Multilevel Finite Element Approximation, B.G. Teubner, Stuttgart, 1994.
[12] R. Stevenson, Piecewise linear (pre-)wavelets on non-uniform meshes, in: W. Hackbusch, G. Wittum (Eds.), Multigrid Methods, Vol. V, Springer, Berlin, 1998, pp. 306–319.
[13] G. Strang, T. Nguyen, Wavelets and Filter Banks, Wellesley-Cambridge Press, Wellesley, 1996.
[14] H. Yserentant, On the multi-level splitting of finite element spaces, Numer. Math. 49 (1986) 371–412.